mathematics

MDPI

Article

Walsh–Hadamard Transform based Non–orthogonal Multiple Access (NOMA) and Interference Rejection Combining in Next-Generation HetNets

M. Rehan Usman [1], M. Arslan Usman [2,3], Soo Young Shin [4,*], Gandeva Bayu Satrya [5], Rizwan A. Naqvi [6], Maria G. Martini [7] and Christos Politis [7]

1 Department of Electrical Engineering, The Superior College (University Campus), 17 Km Raiwind Road, Lahore 54000, Pakistan; rehan.usman@superior.edu.pk
2 Department of Research, Business and Innovation, Kingston University London, Kingston upon Thames KT1 2EE, UK; arslanusman@ieee.org
3 Pangea Connected Ltd., Kingston upon Thames KT1 1BL, UK
4 Department of IT Convergence Engineering, Kumoh National Institute of Technology (KIT), Gumi 39177, Korea
5 School of Applied Sciences, Telkom University, Telekomunikasi St. No. 1, Bandung 40257, Indonesia; gbs@telkomuniversity.ac.id
6 Department of Unmanned Vehicle Engineering, Sejong University, 209, Neungdong-ro, Gwangjin-gu, Seoul 05006, Korea; rizwanali@sejong.ac.kr
7 Faculty of Science, Engineering and Computing, Kingston University London, Kingston upon Thames KT1 2EE, UK; m.martini@kingston.ac.uk (M.G.M.); c.politis@kingston.ac.uk (C.P.)
* Correspondence: wdragon@kumoh.ac.kr

Abstract: In heterogeneous networks (HetNets), non-orthogonal multiple access (NOMA) has recently been proposed for hybrid-access small-cells, promising a manifold network capacity compared to OMA. One of the major issues with the installation of a hybrid-access mechanism in small-cells is the cross-tier interference (intercell interference (ICI)) caused by the macrocell users (MUs) that are unable to establish a connection to the small-cell base station (SBS). In this paper, a joint strategy is proposed for hybrid-access small-cells using the Walsh–Hadamard transform (WHT) with NOMA and interference rejection combining (IRC) to achieve high performance gains and mitigate intercell interference (ICI), respectively. WHT is applied mathematically as an orthogonal variable spreading factor (OVSF) to achieve diversity in communication systems. When applied jointly with NOMA, it ensures better performance gains than the conventional NOMA. It reduces the bit error rate (BER) and enhances subsequent throughput performance of the system. IRC is used at the receiver side for managing the cross-tier interference caused by MUs that are unable to connect to the small-cell base station (SBS) for hybrid-access. The work considers both ideal and nonideal successive interference cancellation (SIC) conditions for NOMA. Mathematical modeling is provided for the proposed joint strategy for HetNets and the results validate it in terms of BER and subsequent user throughput performance, compared to the conventional NOMA approach.

Keywords: heterogeneous networks (HetNets); non-orthogonal multiple access (NOMA); successive interference cancellation (SIC); interference rejection combining (IRC); Walsh–Hadamard transform

Citation: Usman, R.; Usman, A.; Shin, S.Y.; Satrya, G.B.; Naqvi, R.A.; Martini, M.G.; Politis, C.; College , T.S.; Road, K.R.; LHR; et al. Walsh–Hadamard Transform based Non-orthogonal Multiple Access (NOMA) and Interference Rejection Combining in Next-Generation HetNets. *Mathematics* **2021**, *9*, 348. https://doi.org/10.3390/math9040348

Received: 14 December 2020
Accepted: 4 February 2021
Published: 9 February 2021

1. Introduction

Exponential and phenomenal are the most suitable words to describe the increase in user traffic and smart devices in recent years. Such a situation, especially with the introduction of fifth-generation (5G) communication and beyond, has amplified the challenges of meeting high data rate demands and enhanced network coverage, without violating the bandwidth limitations. According to a survey conducted by CISCO, global mobile

data traffic will increase nearly thirteenfold by 2022 [1]. This increment, together with the promises being made by 5G and beyond, shows that efficient bandwidth utilization only will not be enough, leading to comprehensive network restructuring and enhancement requirements. To cope with such issues, one way is to enhance the network heterogeneity by increasing the deployment of base stations (BSs) with different coverage areas, powers, and deployment costs (small-cells).

In recent works, it has indeed been shown multiple times that heterogeneous networks (HetNets) can deliver more bandwidth-efficient communication by deploying low-power BSs called small-cells, i.e., mainly picocells and femtocells, commonly underlaid over a macrocell [2–4]. The concept of small-cells first emerged because of low coverage areas in cellular networks, e.g., basement parking, cell-edge areas, and elevators. Later, small-cells became popular because of their benefits of network traffic offloading and efficient spectrum utilization, especially when deployed in a co-channel environment in a multi-tier cellular network. Where there are advantages of co-channel deployment, at the same time, the main drawback is co-tier and cross-tier interference among multi-tier cells, generally referred to as inter-cell interference (ICI). Furthermore, as aforementioned, 5G and beyond requires increased deployment of small-cells, so dealing with ICI will become more complex and challenging, especially when small-cells are user-owned and mobile. One way to deal with this issue is to provide small-cell access to the interference, creating macrocell users (MUs). Currently, there are three access mechanisms for small-cells, i.e., open, closed, and hybrid-access [4]. The access mechanisms that allow MUs to handover to a small-cell are open and hybrid-access, wherein hybrid-access MUs have limited access to the small-cell. The hybrid-access mechanism is mainly for user-owned small-cells, where resource sharing is used for allowed access to the MUs in a way that they do not affect the quality of small-cell owners referred to as small-cell users (SUs). When it comes to resource sharing, recently, power domain non-orthogonal multiple access (NOMA) is being investigated in HetNets for its benefits [5]. Using NOMA for hybrid-access results in reduced cross-tier interference by letting interfering MUs connect to small-cell base stations (SBSs). This is achieved by forming NOMA pairs between SUs and MUs over the same channel, which leads to another benefit, i.e., very little compromise on SU resources. Some MUs, which may not be able to connect to the SBS using NOMA, can still cause ICI; for such cases, an efficient interference suppression technique is required. A number of interference suppression techniques have been investigated in recent years to handle ICI in HetNets, but very few require limited or no backhaul communication. In this work, we propose a joint strategy for the hybrid-access small-cells to cater to all the issues and scenarios discussed. The joint strategy is presented using the Walsh–Hadamard transform (WHT) with NOMA and the interference rejection combining (IRC) technique, to achieve high performance gains and suppress ICI. The use of WHT improves NOMA performance in terms of user throughput and reduced bit error rate (BER), whereas IRC manages the interference produced by MUs (cross-tier interference) who are denied access to SBS using NOMA

Interference rejection combining is generally used to efficiently combat ICI produced by the neighboring cells [6]. The basic concept of IRC is to simply suppress the unwanted signal information and enhance the wanted part with the help of multiple antenna branches at the receiver. The suppression is done by estimating the covariance matrix that includes the interference signals, and the desired signal is estimated by the channel matrix estimation of the serving cell [6,7]. Estimation of the covariance matrix, which includes the signal information of all interferers, is a complex process, and for this purpose, the machine learning mechanisms discussed in [8,9] can be integrated with the works performed in [6,7]. Figure 1 shows the basic IRC concept. To date, numerous studies have been conducted using IRC for interference suppression. In [10], a low-complexity minimum mean square error (MMSE)-based IRC algorithm was developed for massive MIMO systems. Similarly, a study on the performance of IRC in fifth-generation (5G) networks was performed in [11,12]. According to our knowledge, limited work has been performed

on IRC related to HetNets, especially considering the hybrid-access mechanism, the studies of which include: Investigation of IRC receiver for LTE HetNets [13] and experimental evaluation of IRC in 5G HetNets [14,15].

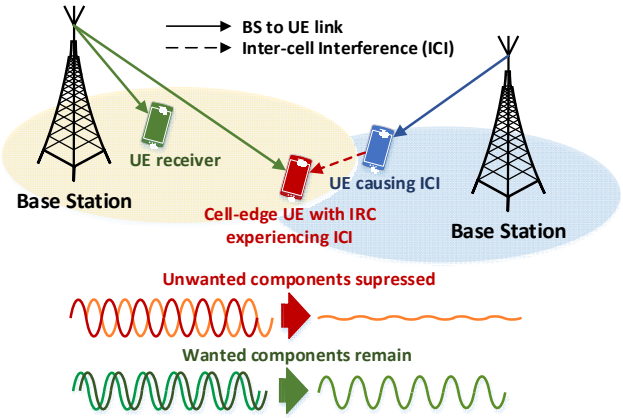

Figure 1. The interference rejection combining (IRC) concept to suppress intercell interference (ICI).

In recent years, NOMA has attracted a substantial amount of research in the field of wireless communication because of its potential to enhance the network capacity manifold [16–20]. NOMA achieves this by multiplexing multiple user transmission signals into a single transmission stream by exploiting the power domain. At the user end, successive interference cancellation (SIC) is used to obtain the required signal information and the rest is discarded. The order of performing SIC is determined by the increasing channel gain of the users [16], i.e., the user with high channel gain performs SIC, generally known as a cell center user (CCU), to decode and cancel out information of the low-gain user, generally referred to as a cell edge user (CEU). Currently, few works have been performed on the use of NOMA in HetNets, which mainly include: NOMA for device-to-device-enabled HetNets [21], spectrum allocation and power control using NOMA in HetNets [5,22], and physical layer security for NOMA-based HetNets [23]. In [24], a contract-theory-based solution is derived for optimizing the use of mobile relays in the cooperative NOMA system, and in [25], a similar solution is proposed for optimizing user association and resource allocation for NOMA in HetNets. Similarly, to use NOMA in HetNets, some game theory and Stackelberg game-based economic approaches are proposed for different purposes in [26–28]. The existing works mainly focus on the integration of NOMA in HetNets or on the user power allocation enhancement with ideal SIC conditions. The main problem with using NOMA in small-cells is that when pairing is performed between the MUs and SUs within a small-cell, depending on the user gain, the performance of paired SUs (considering SUs as high-gain users) may deteriorate in terms of BER, compared to their unpaired state. To address this problem, in this work, WHT is used with NOMA, which overcomes this drawback and ensures better performance gains than the conventional NOMA.

The Walsh–Hadamard transform is used as an orthogonal variable spreading factor (OSVF) to increase the diversity in communication systems [29]. It increases the constellation diversity in the modulation schemes, hence resulting in reduced BER performance and enhanced subsequent user throughput. In recent years, a number of studies have been conducted using the WHT in communication systems; a joint investigation on the WHT and Alamouti scheme was performed in [30], a transceiver design for single carrier frequency division multiple access (SC-FDMA) was proposed using the WHT in [31], and similarly, the WHT was applied on spatial modulation in [32] and on NOMA in [33,34]. To the best of authors' knowledge, to date, no joint strategy has been proposed considering the WHT, NOMA, and IRC in HetNets, particularly under nonideal SIC conditions for

NOMA. To illustrate the concept, a generic HetNet configuration with NOMA-enabled small-cells is shown in Figure 2 and the concept of a WHT-NOMA small-cell is shown in Figure 3. The advantages of the proposed joint strategy have been detailed above. In this framework, the main contributions of this work are summarized as follows:

- Applying the WHT jointly with NOMA and IRC in HetNets will increase the constellation diversity in modulation schemes, hence achieving even better throughput performance and reduced BER compared to the conventional NOMA system. Mathematical modeling is provided for the proposed joint strategy and the results are validated using MATLAB.
- Using IRC in HetNets will combat the interference created at SUs by the MUs that are in the vicinity of the small-cell but are not able to create NOMA pairs with the SUs. In short, interference created by MUs will be suppressed, resulting in better BER and throughput at the SU.

The remainder of this paper is structured as follows. Section 2 describes the mathematical model of the system with the details of the joint strategy, i.e., WHT with NOMA and IRC, considering both ideal and nonideal SIC cases. Section 3 reports the simulation results of the proposed strategy, and final concluding remarks are provided in Section 4.

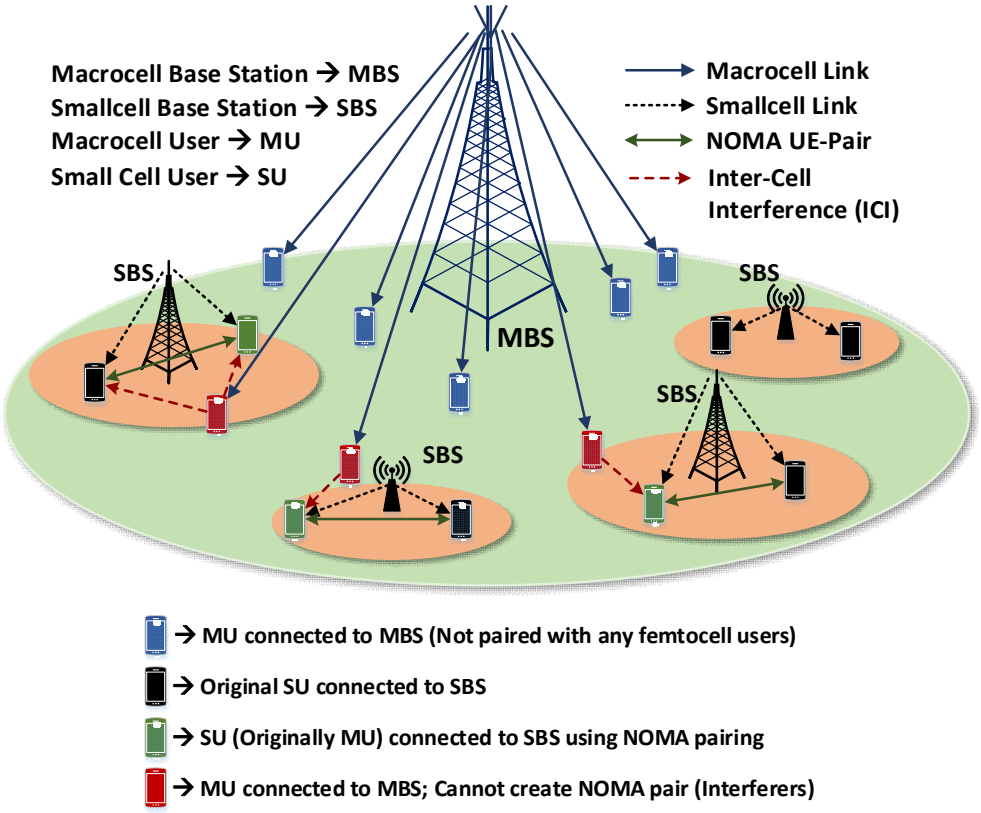

Figure 2. Small-cells deployed in a macrocell with non-orthogonal multiple access (NOMA).

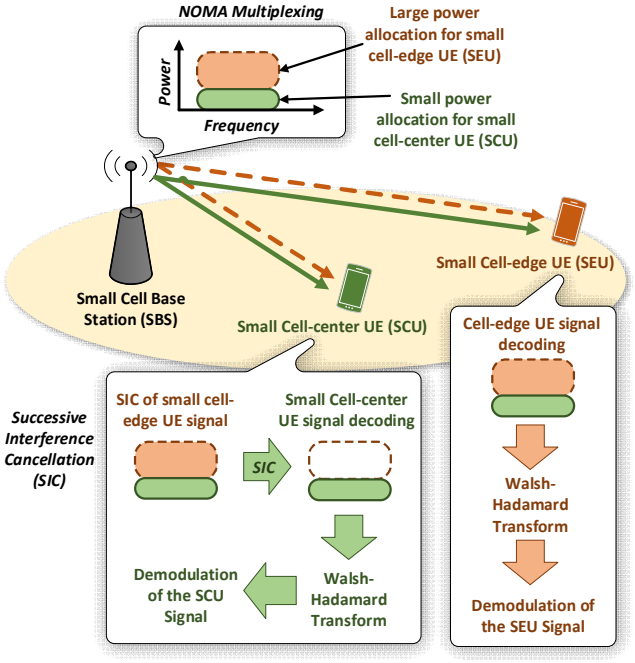

Figure 3. Walsh–Hadamard transform (WHT)-NOMA in a small-cell.

2. System Model

In this section, we present a detailed description of the system model used to develop the system model, starting with conventional NOMA for small-cells, followed by WHT-NOMA in small-cells, then the IRC model for suppression of the interference, caused by MUs that are unable to create NOMA pairs failing to establish connection with the SBS. The general diagram of small-cells deployed in a macrocell with NOMA and ICI is shown in Figure 2, and the transceiver design for the proposed strategy is shown in Figure 4. General notations used in this work are given in Table 1.

Table 1. Notations.

Notations	Description
S	Transmitted Superposition coded signal at b^{th} SBS.
$s_{b,k}$	Signal of k^{th} UE in b^{th} SBS
$\widehat{s}_{b,k}$	Signal information of SEUs with imperfect condition in b^{th} SBS
$s_{b,m}$	Signal of UE-m in b^{th} SBS
$s_{b,k}^{H}$	Signal of the k^{th} UE after the WHT is applied
$\widehat{s}_{b,k}^{H}$	Signal information of SEUs with imperfect conditions at the UE-m served by the b^{th} SBS including WHT
s_{q}^{H}	WHT based signal information of the q^{th} small-cell
s'^{H}_{bm}	Recovered WHT signal using IRC at UE-m in b^{th} SBS
$y_{b,k}$	Received superposition coded signal at the kth UE in b^{th} SBS
$y_{b,m}$	Received signal of UE-m in the b^{th} SBS
N	No of UEs share a common link of the same SBS using NOMA.
N_{SB}	Number of sub-bands in the system
P	Transmission Power
$P_{b,k}$	Total transmission power of the k paired NOMA UEs in the b^{th} SBS
P_{q}	Transmission power of the q^{th} small-cell
P_{SBS}	Serving SBS transmission power
n	Channel Noise
σ^2	Variance
I	Inter-cell Interference
$h_{b,k}$	Transmission channel response from the b^{th} SBS to the k^{th} UE
H_i	WHT matrix with $i = 2^l$ length code $(l \in \mathbb{Z}^+)$

H_q	Complex channel matrix between the q^{th} small-cell and UE
$\propto_k$	Ratio of power assignment to the k^{th} UE
W_q	Precoding weight matrix of the q^{th} small-cell
W_{IRC}	The IRC receiver weight matrix, containing covariance matrix and the estimated channel matrix
$W_{ideal\ IRC}$	Ideal IRC weight matrix at UE-m served by b^{th} SBS
G_{bm}	Composite channel of the b^{th} small-cell
R_{yy}	The covariance matrix respectively
$\boldsymbol{BW}$	Bandwidth
Q	Modulation order of the transmitted signal
T	Throughput

2.1. NOMA in Small-cells

This section of the paper provides the system model for downlink NOMA in hybrid-access small-cells using ideal and nonideal SIC conditions. The section starts with the basic NOMA model and then moves toward the ideal and nonideal SIC part. One important thing to remember is that once the MU becomes an SU, both uplink and downlink are provided by the serving SBS.

In NOMA, the user equipments (UEs) of a superposition-coded signal are considered as paired users. In the existing literature, the maximum number of paired UEs is not yet defined, so for now, it is supposed that the total number of N UEs can share a common link of the same SBS using NOMA. Let us assume that there are $[1 \dots B]$ small-cells underlaid on a macrocell and the b^{th} SBS transmits a superposition-coded signal S for the k paired SUs, given as:

$$S = \sum_{k=1}^{N} s_{b,k}\sqrt{P_{b,k}}\,, \tag{1}$$

where $k \in \{1,2,3, \dots, N\}$, $s_{b,k}$ is the signal of the k^{th} UE, and $P_{b,k}$ is the total transmission power for the k paired UEs. Considering NOMA in small-cells, as aforementioned in Section 1, in user pairing, there are two kinds of UEs, i.e., high gain (small-cell center users (SCUs)) and low gain (small-cell edge users (SEUs)). The ascending value of index k is assigned in descending order of the UE channel gain, i.e., $k = 1$ is the highest-gain user, categorized as SCU, and $k = N$ is the lowest-gain user, categorized as SEU. The received superposition-coded signal at the k^{th} UE in the b^{th} SBS is given as:

$$y_{b,k} = h_{b,k} \times S + n + I. \tag{2}$$

Using (1) and (2) gives:

$$y_{b,k} = h_{b,k} \times \left(\sum_{k=1}^{N} s_{b,k}\sqrt{P_{b,k}}\right) + n + I, \tag{3}$$

where $h_{b,k}$ gives the impulse response of the transmission channel from the b^{th} SBS to the k^{th} UE; we assume in this work a Rayleigh fading channel model, n represents the additive white Gaussian noise (AWGN) with zero mean, and σ^2, and I represent the ICI that is created at the SEU receiver from a nearby MU. Here, P_k is the transmission power associated with the k^{th} UE in the pair given as:

$$P_{b.k} = \frac{\propto_{b,k} \times P_{SBS}}{N_{SB}}, \tag{4}$$

where $\propto_k$ is the ratio of power assignment to the k^{th} UE, P_{SBS} represents the serving SBS transmission power, and the number of sub-bands in the system is given by N_{SB}. In general, $\propto_k$ can take any theoretical value [18].

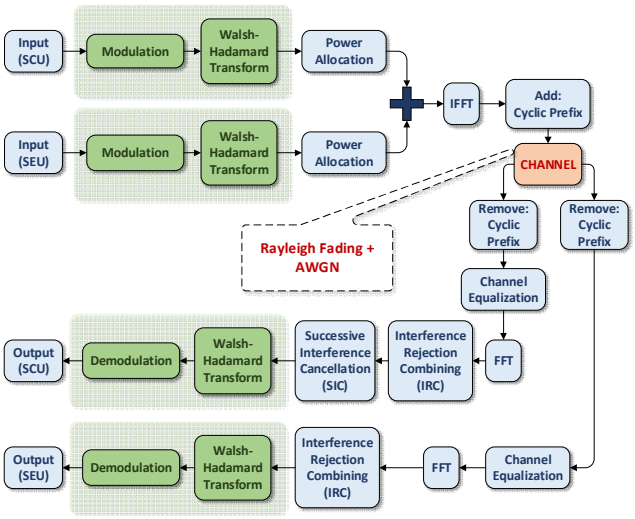

Figure 4. Transceiver block diagram for WHT with joint NOMA and IRC.

Now, as mentioned before, to extract the desired signal information from the received superposition-coded signal of the k paired UEs, a UE-receiver must perform SIC. To do this correctly, it is very important that the UE receiver knows the optimum order of decoding within its paired UEs. This order is determined through the channel-gain of the k paired UEs in a way that only the high-gain users (SCUs) perform SIC to remove the signal information of the low-gain users (SEUs), as shown in Figure 3. Let us consider a high-channel-gain user m, in the k paired UEs, connected to the b^{th} SBS. Then, UE-m must perform SIC to extract its signal by removing the signal information of the low-gain UEs within its pairing. The received signal of UE-m in the b^{th} SBS is given as:

$$y_{b,m} = \underbrace{h_{b,m} \times s_{b,m}\sqrt{P_{b,m}}}_{Wanted\ Signal} + \underbrace{h_{b,m} \times \left(\sum_{k=m+1}^{N} s_{b,k}\sqrt{P_{b,k}}\right)}_{\substack{Unwanted\ Signal:\\ Remove\ using\ SIC}} + \underbrace{n}_{noise} + \underbrace{I}_{ICI}, \quad (5)$$

where, the ICI presented by I consists of two kinds of interference signals, i.e., cross-tier interference and co-tier interference signals. In the co-channel environment, cross-tier interferences occur when the UE of an SBS and a nearby UE of the overlaying macrocell base station (MBS) are allocated the same resource block (RB); similarly, co-tier interferences occur when UEs of neighboring SBSs reuse the same RB. Thus, if there are $[1 \ldots M]$ resource blocks in an MBS and the underlaid small-cells reuse the same RBs, then the ICI created at the UE-m of the serving b^{th} SBS is given as:

$$I = \underbrace{\sum_{a=1}^{M} \lambda_{a,m} h_{a,m} s_a \sqrt{P_a}}_{Cross-tier\ Interference} + \underbrace{\sum_{b' \neq b} \lambda_{b,b'} h^{a}_{b',m} s^{a}_{b',m} \sqrt{P_{b'}}}_{Co-tier\ Interference}, \quad (6)$$

where, s_a and $s^{a}_{b',m}$ are transmitted symbols from the MBS to its MU-a and from SBS-b' to its SU, respectively; $h_{a,m}$ and $h_{b',m}$ are channel responses from MBS and from SBS- b' to UE-m of the serving SBS, respectively; P_a and $P_{b'}$ are transmission powers of the MBS and SBS-b', respectively; $\lambda_{a,m}$ is the RB allocation indicator for cross-tier interference; $\lambda_{a,m} = 1$ when the same RB is being occupied by both SBS and the interfering UE of the MBS; otherwise, $\lambda_{a,m} = 0$. Similarly, $\lambda_{b,b'}$ is the RB allocation indicator for co-tier interference, $\lambda_{b,b'} = 1$ if both serving SBS-b and interfering SBS-b' use the same RB; otherwise, $\lambda_{b,b'} = 0$. Replacing I in (5) gives:

$$y_{b,m} = \underbrace{h_{b,m} \times s_{b,m}\sqrt{P_{b,m}}}_{Wanted\ Signal} + \underbrace{h_m \times \left(\sum_{k=m+1}^{N} s_{b,k}\sqrt{P_{b,k}}\right)}_{\substack{Unwanted\ Signal:\\ Remove\ using\ SIC}} + \underbrace{n}_{noise} + \underbrace{\underbrace{\sum_{a=1}^{M} \lambda_{a,m} h_{a,m} s_a \sqrt{P_a}}_{Cross-tier\ Interference} + \underbrace{\sum_{b' \neq b} \lambda_{b,b'} h^a_{b',m} s^a_{b',m} \sqrt{P_{b'}}}_{Co-tier\ Interference}}_{Inter-cell\ Interference\ (ICI)}. \quad (7)$$

To simplify the problem and as per the existing literature for the NOMA receiver, let us consider a two-user case. Thus, for the two-UE case, the received signal at UE-1 is given by using (5) as:

$$y_{b,1} = \underbrace{h_{b,1} \times s_{b,1}\sqrt{P_{b,1}}}_{Wanted\ Signal} + \underbrace{h_{b,1} \times s_{b,2}\sqrt{P_{b,2}}}_{\substack{Unwanted\ Signal:\\ Remove\ using\ SIC}} + \underbrace{n}_{noise} + \underbrace{I}_{ICI}, \quad (8)$$

where, $s_{b,1}$, $P_{b,1}$, and $h_{b,1}$ are the signal-information, power, and channel-response, respectively, of the high-gain user UE-1, and $s_{b,2}$ and $P_{b,2}$ are signal information and power, respectively, of the low-gain user UE-2. For further investigation of the received signal at the receiver, two cases are considered, i.e., NOMA with perfect and imperfect SIC.

2.1.1. NOMA Receiver with Ideal SIC

In the ideal SIC case, it is assumed that the SCUs have perfect knowledge of the signal information of SEUs, and the channel effects are not considered. This means that the signal information of the SEUs is perfectly cancelled at the SCU by performing SIC. If the SCU user, served by the b^{th} SBS, is UE-m in the k paired UEs, then its received signal, by performing perfect SIC, is given by using (5):

$$s_{b,m} = \left\lfloor \frac{y_{b,m} - \left(\sum_{k=m+1}^{N} s_{b,k}\sqrt{P_{b,k}}\right)}{\sqrt{P_m}} \right\rfloor, \quad (9)$$

where, $\lfloor . \rfloor$ denotes the demodulation and detection of the received signal. In the case of two paired UEs, the SCU is UE-1. Thus, the received signal at UE-1 with the ideal SIC in the b^{th} SBS is given by using (8) and (9):

$$s_{b,1} = \left\lfloor \frac{y_{b,1} - s_{b,2}\sqrt{P_{b,2}}}{\sqrt{P_{b,1}}} \right\rfloor. \quad (10)$$

2.1.2. NOMA Receiver with Nonideal SIC

In this case, the NOMA receiver performance is investigated in a nonideal condition. The case is considered because it is more inclined toward a somewhat practical behavior. Here, the SCU performs SIC in the presence of the channel effects produced by the transmission channel, which in this case, is the Rayleigh fading channel, hence creating a more practical approach than the perfect SIC case. Now, let us suppose that, in the k paired UEs, for the received signal at UE-m, the signal information of the SEUs with imperfect condition in the b^{th} SBS is given from (5) as:

$$\hat{s}_{b,k} = h_{b,k} \times \left(\sum_{k=m+1}^{N} s_{b,k}\sqrt{P_{b,k}}\right) + \underbrace{n}_{noise} + \underbrace{I}_{ICI}, \quad (11)$$

where, n represents the AWGN, I presents the ICI, and $h_{b,k}$ is the Rayleigh fading channel. Then, the signal extraction of UE-m, after performing SIC, is given by using (5) and (11):

$$s_{b,m} = \left\lfloor \frac{y_{b,m} - \widehat{s}_{b,k}}{\sqrt{P_{b,k}}} \right\rfloor. \tag{12}$$

For the case of two paired UEs, the SEU is UE-2 and the SCU is UE-1. Thus, in the received signal at UE-1, the signal information of UE-2, after including the effects of the Rayleigh fading channel and ICI, is given by (11):

$$\widehat{s}_{b,2} = h_{b,2} \times s_{b,2}\sqrt{P_{b,2}} + \underbrace{n}_{noise} + \underbrace{I}_{ICI}. \tag{13}$$

The extracted signal of UE-1 after SIC is given using (12):

$$s_{b,1} = \left\lfloor \frac{y_{b,1} - \widehat{s}_{b,2}}{\sqrt{P_{b,1}}} \right\rfloor. \tag{14}$$

After the description of the NOMA receiver in small-cells with the ideal and nonideal SIC cases, the WHT part is next presented.

2.2. Walsh–Hadamard Transform (WHT)

In this section, the concept of WHT is briefly explained, as it is later used to present WHT-NOMA. In communication systems, a WHT matrix can be applied to the modulation scheme's transmit symbols for achieving constellation diversity. This is because the WHT is used as an orthogonal variable spreading factor (OVSF) to achieve diversity in communication systems. The transform is performed on both sides of the transceiver, i.e., at the transmitter side, multiplying the WHT matrix with the input signal and, similarly, at the receiver side, where the original signal is recovered by multiplying the same WHT matrix with the received signal. The input–output relationship is given by:

$$y = H_i \times S \leftrightarrow S = H_i \times y\,, \tag{15}$$

where, H_i is the WHT matrix with $i = 2^l$ length code $(l \in \mathbb{Z}^+)$ and the input and output signals are given by S and y, respectively. In this transform, every two adjacent rows of a WHT matrix present two perpendicular vectors, which means that they are mutually orthogonal. To provide the WHT matrix illustration, if H presents a Hadamard matrix, then the partitioned matrix is as follows:

$$\begin{bmatrix} H & H \\ H & -H \end{bmatrix}.$$

The observation above provides the general sequence of the WHT matrix as:

$$H_1 = [1], H_2 = \frac{1}{\sqrt{2}}\begin{bmatrix} 1 & 1 \\ 1 & -1 \end{bmatrix}, \ldots, H_{i=2^l} = \frac{1}{\sqrt{i}}\begin{bmatrix} H_{j=2^{l-1}} & H_{j=2^{l-1}} \\ H_{j=2^{l-1}} & -H_{j=2^{l-1}} \end{bmatrix}, \tag{16}$$

where, the order of the Hadamard matrix is given by j, which is used for deriving the matrix H_i, and $1/\sqrt{i}$ presents the normalization factor. Let us suppose that the modulator-output data's complex constellation points (such as phase shift keying (PSK) or quadrature amplitude modulation (QAM)) are: $x_{data} = [x_1\, x_2\, x_3 \cdots x_n]$; then, applying the WHT matrix yields:

$$S_H = x_{data} \times H_i\,, \tag{17}$$

where, S_H is recoverable using (15), i.e., by applying the WHT matrix of the same order at the receiver side. The above process can be easily understood via the following example: Let us assume $x_{data} = [x_1 \ x_2]$ is the given data with the WHT matrix H_2, i.e., matrix of order 2. Then, by using (16) and (17), we get:

$$S_H = [x_1 \ x_2] \times \frac{1}{\sqrt{2}} \begin{bmatrix} 1 & 1 \\ 1 & -1 \end{bmatrix} = \frac{1}{\sqrt{2}} [s_1 \ s_2], \tag{18}$$

$$s_1 = \frac{1}{\sqrt{2}}(x_1 + x_2), \tag{19}$$

$$s_2 = \frac{1}{\sqrt{2}}(x_1 - x_2). \tag{20}$$

where, s_1 and s_2 are the derived resultant points after WHT matrix application in (19) and (20), respectively. These symbols are then transmitted instead of the original data. As aforementioned, that WHT is applied on modulator-output data, so if we consider a typical quadrature phase shift keying (QPSK) transmitter, then we obtain four constellation points, i.e., 00, 01, 10, and 11 (example). The application of the WHT on these points is shown in Table 2, where x_1 and x_2 are the modulation points with their complex constellation points $\hat{x}_1$ and $\hat{x}_2$, respectively. After applying the WHT, the new constellation points are presented as s_1 and s_2, respectively.

To recover the data, a WHT matrix of the same order is applied to the received data at the receiver side. The process is given as:

$$Y_H = [s_1 \ s_2] \times \begin{bmatrix} 1 & 1 \\ 1 & -1 \end{bmatrix},$$

$$Y_H = [x_1 + x_2 \ x_1 - x_2] \times \begin{bmatrix} 1 & 1 \\ 1 & -1 \end{bmatrix},$$

$$Y_H = \begin{bmatrix} x_1 + x_2 + x_1 - x_2 \\ x_1 + x_2 - x_1 + x_2 \end{bmatrix} = \begin{bmatrix} 2x_1 \\ 2x_2 \end{bmatrix} \tag{21}$$

where (21) shows the diversity achieved by applying WHT.

After this illustration of the use of the WHT model in communication systems, we next describe NOMA with WHT in small-cells.

Table 2. New Constellation Points After Application of WHT.

x_1	$\hat{x}_1$	x_2	$\hat{x}_2$	$s_1 = \frac{1}{\sqrt{2}}(x_1 + x_2)$	$s_2 = \frac{1}{\sqrt{2}}(x_1 - x_2)$
00	1.0 + 0.0j	00	1.0 + 0.0j	1.4142 + 0j	0 − 0j
00	1.0 + 0.0j	01	0.0 + 1.0j	0.7071 + 0.7071j	0.7071 − 0.7071j
00	1.0 + 0.0j	11	−0.0 − 1.0j	0.7071 − 0.7071j	0.7071 + 0.7071j
00	1.0 + 0.0j	10	−1.0 + 0.0j	0 + 0j	1.4142j − 0j
01	0.0 + 1.0j	00	1.0 + 0.0j	0.7071 + 0.7071j	−0.707z1 + 0j
01	0.0 + 1.0j	01	0.0 + 1.0j	0 + 1.4142j	0 − 0j
01	0.0 + 1.0j	11	−0.0 − 1.0j	0 − 0j	0 + 1.4142j
01	0.0 + 1.0j	10	−1.0 + 0.0j	−0.7071 + 0.7071j	0.7071 + 0.7071j
10	−0.0 − 1.0j	00	1.0 + 0.0j	0.7071 − 0.7071j	−0.7071 − 0.7071j
10	−0.0 − 1.0j	01	0.0 + 1.0j	0 − 0j	0 − 1.4142j
10	−0.0 − 1.0j	11	−0.0 − 1.0j	0 − 1.4142j	0 − 0j
10	−0.0 − 1.0j	10	−1.0 + 0.0j	−0.7071 − 0.7071j	0.7071 − 0.7071j
11	−1.0 + 0.0j	00	1.0 + 0.0j	0 + 0j	−1.4142 − 0j

11	−1.0 + 0.0j	01	0.0 + 1.0j	−0.7071 + 0.7071j	−0.7071 − 0.7071j
11	−1.0 + 0.0j	11	−0.0 − 1.0j	−0.7071 − 0.7071j	−0.7071 + 0.7071j
11	−1.0 + 0.0j	10	−1.0 + 0.0j	−1.4142 + 0j	0 − 0j

2.3. WHT-NOMA in Small-cells

This part provides the description of the proposed NOMA with the WHT technique. The block-diagram of the proposed technique is provided in Figure 3. If the superposition-coded signal at the b^{th} SBS transmitter is given by (1), then after the WHT application, it is given as:

$$S = \sum_{k=1}^{N} s_{b,k}^{H} \sqrt{P_{b,k}}, \tag{22}$$

where, $s_{b,k}^{H}$ represents the signal of the k^{th} UE after the WHT is applied. Similarly, at the receiver side, using Equation (3), the received signal at the k^{th} user is given as:

$$y_{b,k} = h_{b,k} \times \left(\sum_{k=1}^{N} s_{b,k}^{H} \sqrt{P_{b,k}} \right) + n + I, \tag{23}$$

where, $h_{b,k}$ is the channel response, assuming a Rayleigh fading channel, n represents noise, and I presents the ICI, with the noise considered in this work as AWGN with zero mean and variance σ^2.

In WHT-NOMA, for the m^{th} UE case in k paired UEs served by the b^{th} SBS, the received signal of high-gain user UE-m in (5) without performing SIC can be written as:

$$y_{b,m} = \underbrace{h_{b,m} \times s_{b,k}^{H} \sqrt{P_{b,m}}}_{Wanted\ Signal} + \underbrace{h_{b,m} \times \left(\sum_{k=m+1}^{N} s_{b,k}^{H} \sqrt{P_{b,k}} \right)}_{\substack{Unwanted\ Signal: \\ Remove\ using\ SIC}} + \underbrace{n}_{noise} + \underbrace{I}_{ICI}, \tag{24}$$

where I is given in (6). Like the two-UE case in WHT-NOMA, the received signal at UE-1, served by the b^{th} SBS, without SIC will be given by using (24) as:

$$y_{b,1} = \underbrace{h_{b,1} \times s_{b,1}^{H} \sqrt{P_{b,1}}}_{\text{Wanted Signal}} + \underbrace{h_{b,1} \times s_{b,2}^{H} \sqrt{P_{b,2}}}_{\substack{\text{Unwanted Signal:} \\ \text{Remove using SIC}}} + \underbrace{n}_{\text{noise}} + \underbrace{I}_{\text{ICI}}. \tag{25}$$

Here as well, just like conventional NOMA in small-cells, two cases are considered for SIC at the SU receiver, i.e., WHT-NOMA with perfect and imperfect SIC.

2.3.1. WHT-NOMA Receiver with Ideal SIC

Just like the ideal SIC part for the conventional NOMA receiver, it is assumed that the SCU has perfect knowledge of the signal information of SEUs. The SCU cancels the signal information of the SEUs completely from the combined signal using SIC. Then, in the WHT-NOMA receiver, the signal of high-gain user UE-m, in the k paired UEs, served by the b^{th} SBS is retrieved using (25) as:

$$s_{b,m} = \left\lfloor \left(\frac{y_{b,m} - \left(\sum_{k=m+1}^{N} s_{b,k}^{H} \sqrt{P_{b,k}} \right)}{\sqrt{P_{b,m}}} \right) \times H_i \right\rfloor, \tag{26}$$

where, H_i is the WHT matrix of the same order i as used for the transmitter, and $\lfloor . \rfloor$ denotes the demodulation and detection of the received signal. In the two-paired-UE case, to retrieve the signal of high-gain user UE-1, (26) is written as:

$$s_{b,1} = \left\lfloor \left(\frac{y_{b,1} - s_{b,2}^{H} \sqrt{P_{b,2}}}{\sqrt{P_{b,1}}} \right) \times H_i \right\rfloor. \quad (27)$$

2.3.2. WHT-NOMA Receiver with Nonideal SIC

In this case also, just like the nonideal SIC part for the conventional NOMA receiver in subsection 2.1, the SCU performs SIC in the presence of the channel effects produced by the transmission channel, i.e., the Rayleigh fading channel. In this case, for WHT-NOMA, the signal information of SEUs at the UE-m served by the b^{th} SBS is given using (24) as:

$$\hat{s}_{b,k}^{H} = h_{b,k} \times \left(\sum_{k=m+1}^{N} s_{b,k}^{H} \sqrt{P_{b,k}} \right) + \underbrace{n}_{noise} + \underbrace{I}_{ICI}, \quad (28)$$

where, n, I, and $h_{b,k}$ represent the AWGN, ICI, and the Rayleigh fading channel, respectively. Then, in the WHT-NOMA case, the signal information of UE-m, served by b^{th} SBS, is extracted using (24) and (28):

$$s_{b,m} = \left\lfloor \left(\frac{y_{b,m} - \hat{s}_{b,k}^{H}}{\sqrt{P_{b,k}}} \right) \times H_i \right\rfloor. \quad (29)$$

For the two-UE-pair case in WHT-NOMA, the signal information of UE-2 at UE-1, after including the effects of the Rayleigh fading channel, is given using (28) as:

$$\hat{s}_{b,2}^{H} = h_{b,2} \times s_{b,2}^{H} \sqrt{P_{b,2}} + \underbrace{n}_{noise} + \underbrace{I}_{ICI}. \quad (30)$$

The UE-1's received signal, after SIC, can be extracted using (25) and (30) given as:

$$s_{b,1} = \left\lfloor \left(\frac{y_{b,1} - \hat{s}_{b,2}^{H}}{\sqrt{P_{b,1}}} \right) \times H_i \right\rfloor, \quad (31)$$

where, as aforementioned, H_i is the WHT matrix of the same order i, as used for the SBS transmitter, and $\lfloor . \rfloor$ represents the demodulation and detection of the received signal.

After the description of the WHT-NOMA receiver for both ideal and nonideal SIC cases, the description of the IRC model is next presented.

2.4. IRC Receiver to Suppress ICI in Small-cells

This part of the paper presents the system model for the IRC receiver in small-cells, continued with the former WHT-NOMA. The block diagram for the WHT with joint NOMA and IRC is given in Figure 4. As mentioned in Section 1, that IRC receiver needs to know the interference signals and the desired signal, i.e., the correct covariance matrix estimation that includes the information of interfering signals, and the channel matrix estimation of the serving cell, respectively. Thus, to achieve accurate estimates of these matrices using IRC, efficient estimation schemes are required [6]. In the current high-end wireless networks, the serving cells' channel matrix estimation is possible using the downlink reference signals (RSs). The covariance matrix can be estimated using the RS-based scheme proposed in the 3GPP release R1-111562 [35]. This scheme extracts the serving cell's portion, and the noise and interference portion from the covariance matrices. The former portion, i.e., attaining covariance matrix of the serving cell, can be achieved via the phases and channel amplitudes of the serving cell, which can be estimated by the RS of the serving cell. On the contrary, the latter part, i.e., the covariance matrix estimation that includes only the noise and interference, can be achieved by the subtraction of replica

symbols of the serving cell, based on the estimated channel matrix and the known RS sequence, from the received RS signals. As IRC is particularly used for the interference suppression, the estimation accuracy of the latter is more important than the former. In this work, for simplicity, the ideal IRC scenario is used where the composite signal information of the interferers is known at the IRC performing receiver.

To present the system model for IRC, the model used is the same as for the NOMA in small-cells, but for a better understanding, it is presented here from the perspective of multiple antenna receivers, as IRC can suppress the ICI if the number of receiver antennas is higher than the desired data streams [6]. The IRC model developed in this work is based on the work performed in [6]. Considering that N_{Rx} is the number of receiver antenna branches and the total number of cells, including the macro and small-cells, is given by N_{Cell}, then the received signal is given as:

$$y = \sum_{q=1}^{N_{cell}} H_q W_q s_q^H \sqrt{P_q} + n, \tag{32}$$

where, H_q is the complex channel matrix between the q^{th} small-cell and UE, s_q^H is the WHT-based signal information of the q^{th} cell, P_q is the transmission power of the q^{th} small-cell, W_q is the precoding weight matrix of the q^{th} small-cell, and n is the N_{Rx}-dimensional noise. Considering that the b^{th} SBS is serving a high-gain UE-m from the total k NOMA-paired UEs, the recovered WHT signal after successful removal of the ICI using IRC at the UE-m, i.e., s'^H_{bm}, is detected using the $(N_{stream} \times N_{Rx})$ receiver weight matrix $W_{Rx,bm}$, where N_{stream} is the total number of streams received at the UE. The desired signal is given as:

$$s'^H_{bm} = W_{Rx,bm} y. \tag{33}$$

The IRC receiver weight matrix, which contains the covariance matrix with interference information and the estimated channel matrix, is given as:

$$W_{IRC} = W_{Rx,bm} = \sqrt{P_{bm}} G_{bm} R_{yy}^{-1}, \tag{34}$$

$$G_{bm} = H_{bm} W_{bm}, \tag{35}$$

where, G_{bm}, P_{bm}, and R_{yy} denote the composite channel of the b^{th} small-cell, the transmission power of the serving b^{th} SBS, and the covariance matrix, respectively. Using W_{IRC} in (34) instead of $W_{Rx,bm}$ in (33) gives us the desired signal by supressing the interference information. If the ideal IRC case is considered, then composite channels, i.e., from serving cell and all interferers, are known at the receiver, so the ideal IRC weight matrix at the UE-m served by b^{th} SBS will be given by using (34) as:

$$W_{ideal\ IRC} = \underbrace{G_{bm}^{H'} \sqrt{P_{bm}}}_{\text{Serving SBS part}} \left(\underbrace{\sum_{q=1}^{N_{cell}} G_q G_q^{H'} \sqrt{P_q}}_{\text{interferers part}} + \underbrace{n}_{\text{noise}} \right)^{-1}, \tag{36}$$

where, $G_q^{H'}$ is the Hermitian transpose of the composite channel. Using the ideal IRC weight matrix, i.e., $W_{ideal\ IRC}$, instead of the receiver weight matrix $W_{Rx,bm}$ supresses the interference caused by other cells. However, considering that the composite channels from other cells are not known at the receiver, the covariance matrix that includes ICI infor-

mation needs to be estimated; for this reason, 3GPP has introduced a demodulation reference signal (DM-RS) approach [35]. Based on this model, IRC suppresses interference intelligently and limited backhaul communication is required, resulting in low-latency communication; nevertheless, this is not included in the scope of this work.

2.4. User Throughput Performance

The user throughput calculation for the proposed model in this work, i.e., WHT-NOMA and IRC, is based on BER performance [36]. As user throughput and BER are related to each other, in this paper, in both cases, i.e., conventional NOMA and WHT-NOMA, throughput is calculated based on the BER performance as follows:

$$T = (1 - BER) \times \boldsymbol{BW} \times log_2(Q), \quad (37)$$

where, $\boldsymbol{BW}$ is the bandwidth and Q is the modulation order of the transmitted signal.

After a detailed description of the system model, the next section gives the simulation results conducted to validate the presented work in this paper.

3. Results and Discussion

This section provides simulation results for the presented WHT-based joint NOMA and IRC in comparison with the conventional NOMA scheme using perfect and imperfect SIC conditions. The results are discussed in terms of BER, and subsequent user throughput performance. The simulations are carried out in MATLAB using two case scenarios, i.e., 1) investigating the performance of SU when it pairs with an interfering MU in terms of BER and throughput performance using conventional NOMA and WHT-NOMA, 2) performance of SCUs and SEUs in terms of user throughput and BER, considering WHT-NOMA with IRC to suppress the ICI effects. Both scenarios incorporate the ideal and non-ideal SIC conditions for NOMA, where the nonideal condition includes noise and channel effects.

As NOMA has not been standardized yet, the simulation parameters in this work follow the LTE standard as stated in the 3GPP specifications. For the same reason, the basic signal waveform used for the simulations is also taken from the LTE standard. The simulation parameters are defined in Table 3. For simplicity, a single SBS is considered, deployed under an MBS. For the WHT matrix, the same order is used as for the used modulation scheme, e.g., for binary phase shift keying (BPSK) modulation, the order of the WHT matrix is 2 and for QPSK modulation, the order of the WHT matrix is 4. The results according to the scenarios are given as follows.

Table 3. Simulation Parameters.

Bandwidth	1.4 MHz
Radio access scheme	OFDM
Subcarrier separation	15 kHz
Number of Subcarriers	600 (50 RBs)
FFT size	2048
Subframe length	1.0 ms (14 OFDM symbols)
Symbol Duration	66.67 μs + CP: 4.69 μs
Data modulation for SCU	BPSK, QPSK, QAM, 8-QAM
Data modulation for SEU	BPSK, QPSK, QAM, 8-QAM
User Power for NOMA	SCU = 0.4, 0.2, SEU = 0.6, 0.8
Channel/Noise	Rayleigh fading channel/AWGN
Maximum Doppler frequency	5.55 Hz
FFT timing detection	Ideal
Inter-Cell Interference (ICI)	1 interferer = 20 dBm

3.1. Scenario 1

In this scenario, BER and throughput performance of an SU are investigated before and after pairing it with the interfering MU. To measure the performance, for simplicity, a single SU is considered as a high-gain UE with a single interfering MU (interfering signal strength = 20 dBm). Further, the unpaired SU contains ICI effects produced by the interfering MU. To manage the situation, SU pairs with the MU using power domain NOMA suppressing the ICI. The results are generated using power allocation as SU (SCU) = 0.4 and MU (SEU) = 0.6, where the total power is equal to 1, i.e., $P_{SCU} + P_{SEU} = 1$. The scenario is shown in Figure 5a and the results are presented in Figures 6–13.

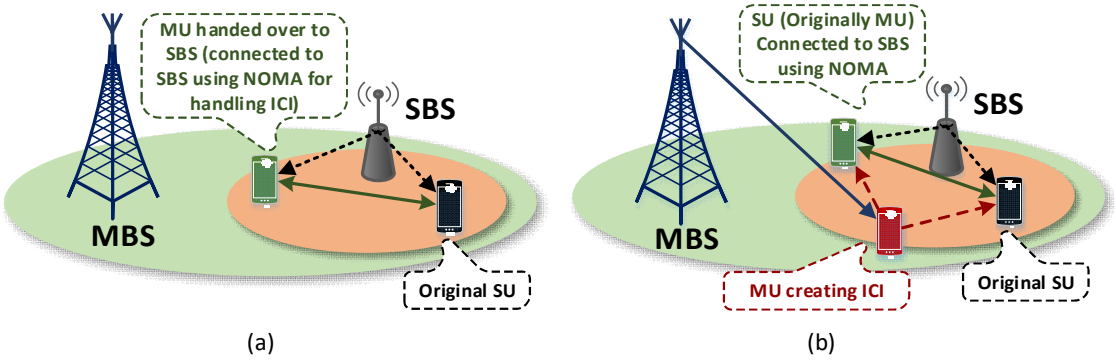

Figure 5. Simulation Scenarios: (**a**) Interfering MU connected to SBS using NOMA; (**b**) two NOMA paired SUs with one interfering MU.

3.1.1. BER Performance

This part shows the BER performance of a high-gain SU, before and after pairing it with the interfering MU, using different modulation schemes. The results are provided in comparison of conventional NOMA with WHT-NOMA shown in Figures 6 to 9.

In Figure 6, the results are derived using BPSK modulation. It can be observed from this investigation that using NOMA, the BER performance of SU deteriorates after pairing with the interfering MU, even after performing SIC, compared to its unpaired state. In terms of hybrid-access small-cells, this deterioration is unacceptable as SUs are the owners of the small-cell. Thus, to deal with the situation, WHT is applied to NOMA. It can be observed that using WHT-NOMA, for the paired SUs, there is a performance gain of almost 5–10 dB in SNR for different BER values in both perfect and imperfect SIC conditions compared to the conventional NOMA. Thus, it can be seen that using WHT reduces the BER significantly, resulting in an even better BER performance of the paired SU compared to its unpaired state. A similar trend can be seen in Figure 7, where QPSK modulation is used with the WHT matrix of order 4 (H_4 from equation (16)).

The simulations in Figures 8 and 9 are derived using the higher-order modulation schemes, i.e., QAM and 8-QAM, respectively. It can be observed that the trend in performance gains for WHT-NOMA is similar to the results in Figures 6 and 7, i.e., approximately 5–10 dB in SNR for different BER values, compared to the conventional NOMA. Here also, the results signify the importance of using WHT-NOMA in small-cells by showing even better BER performance of the paired SU, compared to its unpaired state.

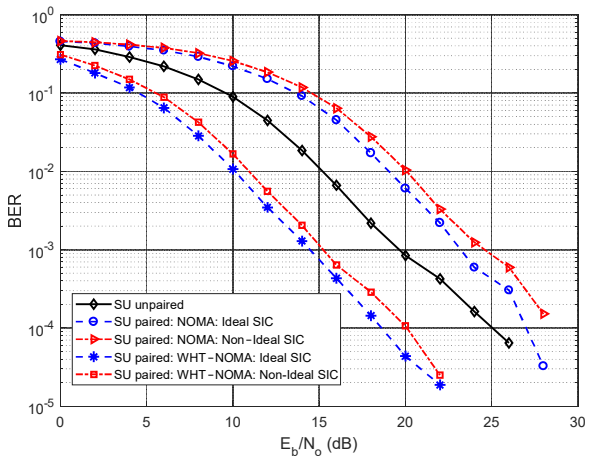

Figure 6. BER performance using BPSK modulation; NOMA Vs. WHT–NOMA, power allocation: SU (SCU) = 0.4 and MU (SEU) = 0.6.

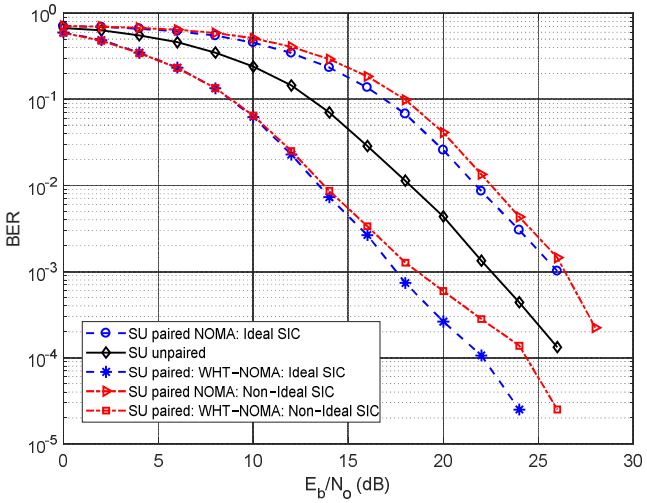

Figure 7. BER performance using QPSK modulation; NOMA Vs. WHT–NOMA, power allocation: SU (SCU) = 0.4 and MU (SEU) = 0.6.

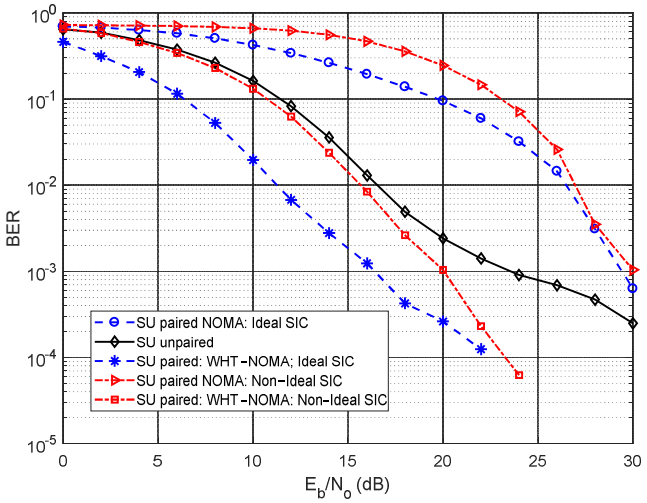

Figure 8. BER performance using QAM modulation; NOMA Vs. WHT–NOMA, power allocation: SU (SCU) = 0.4 and MU (SEU) = 0.6.

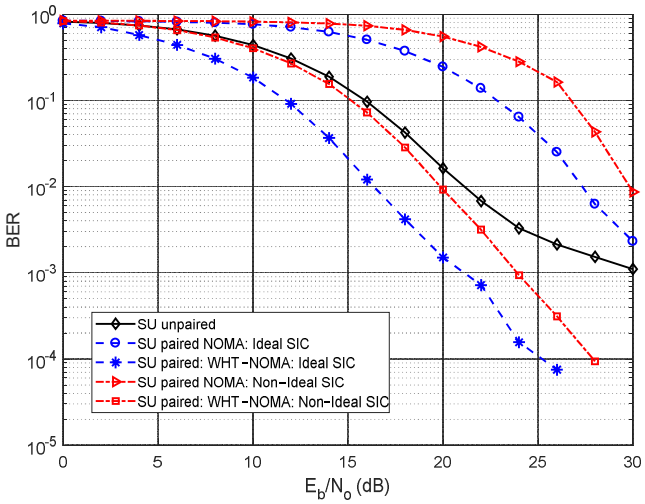

Figure 9. BER performance using 8–QAM modulation; NOMA Vs. WHT–NOMA, power allocation: SU (SCU) = 0.4 and MU (SEU) = 0.6.

3.1.2. Throughput Performance

This part shows the throughput performance of the high-gain SU in Figure 5a, before and after pairing it with the interfering MU, using different modulation schemes. The results are derived using the BER performance of SU, presented above. These simulations are also provided in comparison of conventional NOMA with WHT-NOMA given in Figures 10–13.

In Figure 10, the results are derived using BPSK modulation. The observation in this figure yields that using NOMA, the throughput performance of SU degrades with pairing, even after performing SIC, compared to its unpaired state. As aforementioned, in hybrid-access small-cells, throughput degradation, because of the nonsubscriber presence, is unacceptable as SUs are the rightful owners or subscribers of the small-cell. Thus, to deal with the situation, it can be seen that using WHT-NOMA, the throughput performance increases in both perfect and imperfect SIC conditions compared to the conventional NOMA. The paired SUs' performance is even better than its unpaired state. At 10 dB SNR, using WHT-NOMA, compared to conventional NOMA, it can be observed that for paired SU, there is an increase of approximately 0.3 Mbps using the ideal SIC and 0.34 Mbps using nonideal SIC. Furthermore, it can be seen that the paired SUs' throughput performance compared to its unpaired state also increases using WHT-NOMA, i.e., 0.13 Mbps increase in throughput using ideal SIC and 0.11 Mbps increase using nonideal SIC conditions. A similar trend can be seen in Figure 11, where QPSK modulation is used with the WHT matrix of order 4 (H_4 from (16)).

The results in Figures 12 and 13 are derived using the higher-order modulation schemes, i.e., QAM and 8-QAM, respectively, and are based on the BER performance shown in Figures 8 and 9, respectively. It can be observed that the trend in throughput performance using WHT-NOMA is similar to the trend followed in Figures 10 and 11. For example, in Figure 13, at 10 dB SNR using WHT-NOMA, compared to conventional NOMA, the throughput of paired SU increases approximately 2.25 Mbps with the ideal SIC and 2.22 Mbps with nonideal SIC. It even exceeds the throughput of its unpaired state, i.e., approximately 1.30 Mbps.

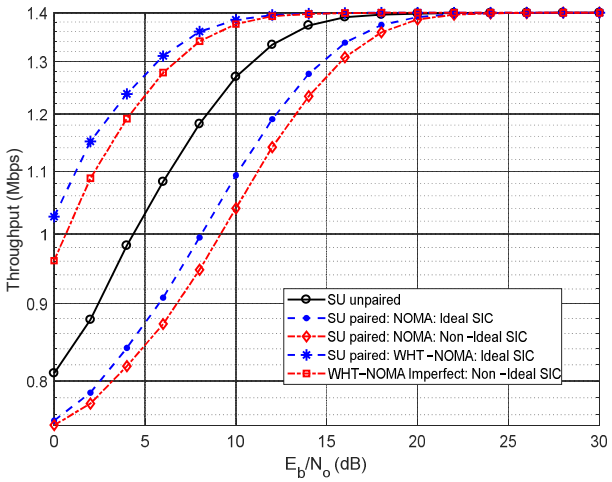

Figure 10. Throughput performance using BPSK modulation; NOMA Vs. WHT–NOMA, power allocation: SU (SCU) = 0.4 and MU (SEU) = 0.6.

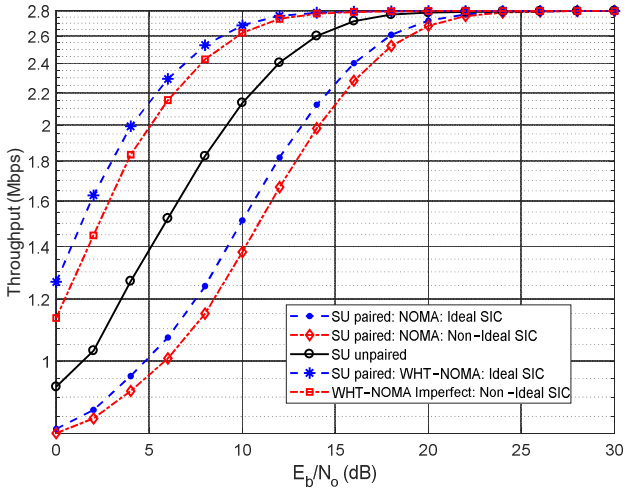

Figure 11. Throughput performance using QPSK modulation; NOMA Vs. WHT–NOMA, power allocation: SU (SCU) = 0.4 and MU (SEU) = 0.6.

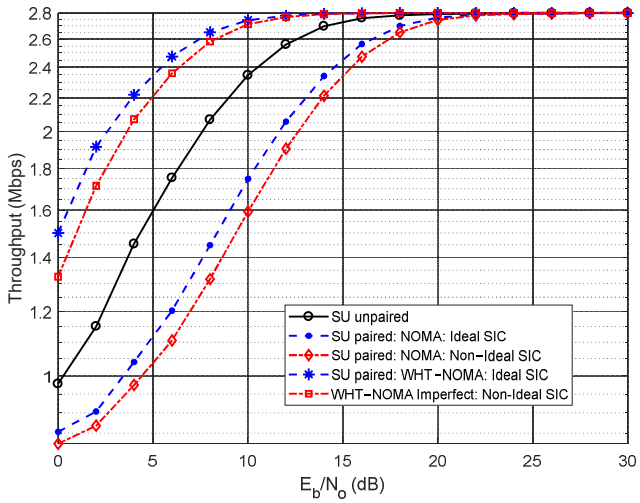

Figure 12. Throughput performance using QAM modulation; NOMA Vs. WHT–NOMA, power allocation: SU (SCU) = 0.4 and MU (SEU) = 0.6.

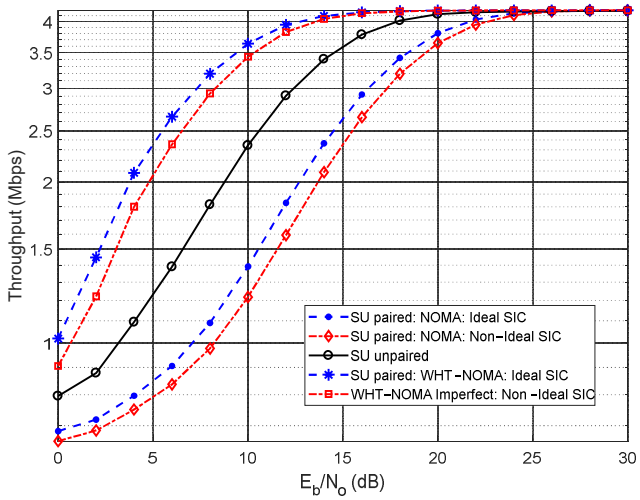

Figure 13. Throughput performance using 8–QAM modulation; NOMA Vs. WHT–NOMA, power allocation: SU (SCU) = 0.4 and MU (SEU) = 0.6.

3.2. Scenario 2

In this scenario, the BER and throughput performance of SCU and SEU are investigated using WHT-NOMA with IRC compared to conventional NOMA with and without IRC. To measure the performance, for simplicity, a two-UE-pair case is used, i.e., an SCU (high-gain user) paired with a SEU (low-gain user). Both SCU and SEU experience ICI from a MU that is not able to connect to the SBS; the interfering signal strength is considered as 20 dBm. To manage the situation, IRC is used for ICI suppression at both SCU and SEU. The results are generated using power allocation as SCU = 0.2 and SEU = 0.8, where the total power is equal to 1, i.e., $P_{SCU} + P_{SEU} = 1$. The scenario is shown in Figure 5b and the results are presented in Figures 14–21.

3.2.1. BER Performance

This part shows the BER performance of both SCU and SEU using scenario 2 for different modulation schemes. The results are given in Figures 14–17.

In Figure 14, the BER results are derived using BPSK modulation for both SUs, i.e., SCU and SEU, using WHT-NOMA with IRC compared to conventional NOMA with and without IRC. Similar to scenario 1, it can be observed that using WHT-NOMA results in a performance gain of approximately 5–10 dB in SNR for different BER values for both SUs, i.e., SCU and SEU, compared to the conventional NOMA. The receiver performance of WHT-NOMA is better than conventional NOMA for both ideal and nonideal SIC cases. As the SCU is the high-gain user with low power assignment, and further, the SIC is also performed by SCU, it can be seen that the performance of SEU is better compared to SCU. Furthermore, it can also be observed that using IRC results in reduced BER for both SCU and SEU, in all cases showing the suppression of ICI caused by the interfering MU. A similar trend can be observed in Figure 15 where QPSK modulation is used with a WHT matrix of order 4 (H_4 from (16)).

For the higher-order modulation schemes, i.e., QAM and 8-QAM, the BER results for scenario 2 are shown in Figures 16 and 17, respectively. It can be observed that these results also follow the same trend as in Figures 14 and 15, i.e., approximately 5–10 dB performance gain in SNR for different values of BER using WHT-NOMA for both SCU and SEU, compared to conventional NOMA. This shows that there is a significant receiver performance gain in terms of the BER for WHT-NOMA compared with the conventional NOMA, and the use of IRC suppresses the ICI, especially at higher SNR values.

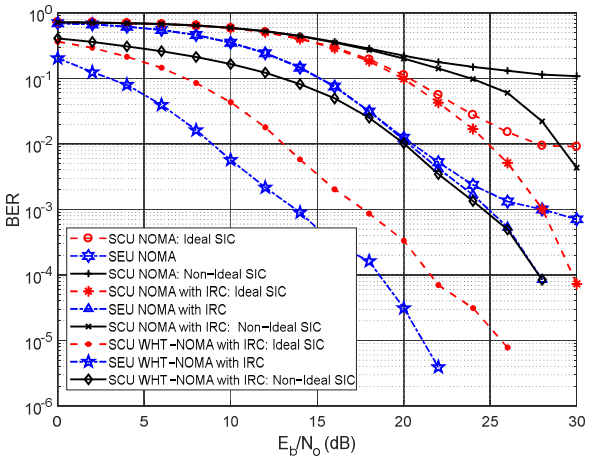

Figure 14. BER performance with IRC using BPSK modulation; NOMA Vs. WHT–NOMA, power allocation: SCU = 0.2 and SEU = 0.8.

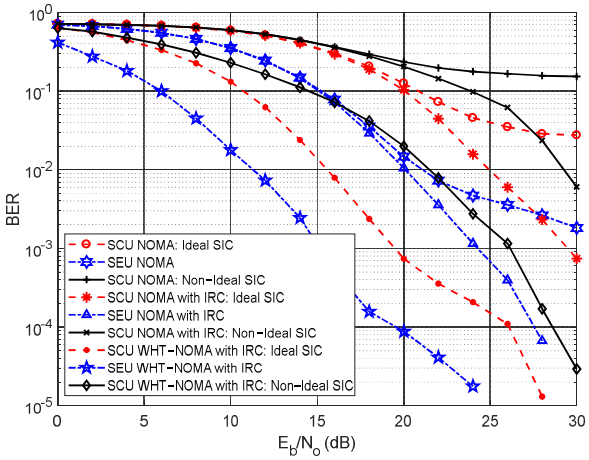

Figure 15. BER performance with IRC using QPSK modulation; NOMA Vs. WHT–NOMA, power allocation: SCU = 0.2 and SEU = 0.8.

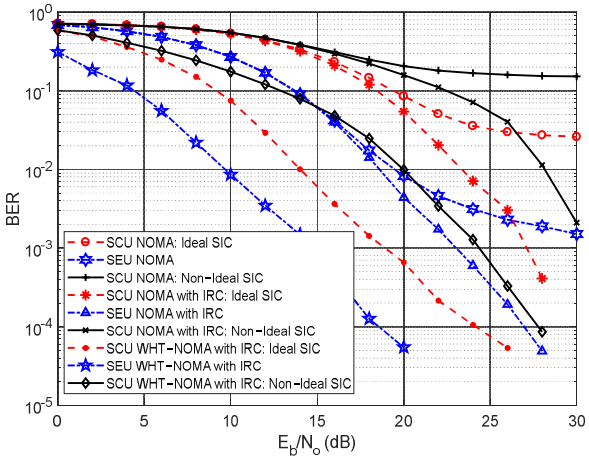

Figure 16. BER performance with IRC using QAM modulation; NOMA Vs. WHT–NOMA, power allocation: SCU = 0.2 and SEU = 0.8.

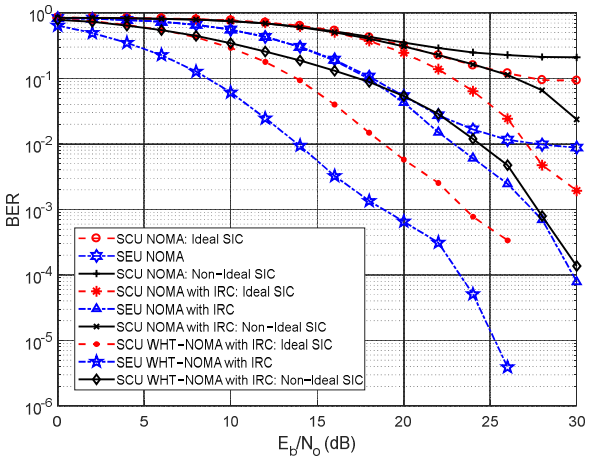

Figure 17. BER performance with IRC using 8–QAM modulation; NOMA Vs. WHT–NOMA, power allocation: SCU = 0.2 and EU = 0.8.

3.2.2. Throughput Performance

This part shows the throughput performance of both SUs, i.e., SCU and SEU, using scenario 2 for different modulation schemes. The results are given in Figures 18 to 21 and are based on the BER performance results in Figures 14–17, respectively.

In Figure 18, the results are shown for conventional NOMA and WHT-NOMA with IRC using BPSK modulation. Like the results in scenario 1, it can be observed that using WHT-NOMA yields better throughput performance than conventional NOMA for both SCU and SEU. The receiver performance of WHT-NOMA is better for both ideal and non-ideal SIC cases. For example, it can be observed that at 10 dB SNR, using WHT-NOMA and IRC results in an approximately 0.24 Mbps throughput increase for SEU compared to conventional NOMA with IRC. The results also show that using IRC with WHT-NOMA or conventional NOMA increases the throughput of both SCU and SEU in all cases, showing ICI suppression. The throughput performance because of IRC becomes even better at high SNR values, e.g., at 20 dB SNR, using IRC with conventional NOMA results in an approximately 0.05 Mbps throughput increase for SCU compared to the conventional NOMA without IRC. A similar trend is observed for all cases in Figure 19 where QPSK modulation is used considering a Hadamard matrix of order 4.

Like the previous cases, the results in Figures 20 and 21 are produced for higher-order modulations, i.e., QAM and 8-QAM. These results also follow the same trend of throughput performance as followed by BPSK and QPSK in Figures 18 and 19, i.e., the throughput performance of both SUs, i.e., SCU and SEU, enhances with the use of WHT with NOMA compared to the conventional NOMA. Furthermore, the use of IRC suppresses ICI at the SCU and SEU receiver, yielding better throughput performance, especially at higher SNR values as visible from results in both figures.

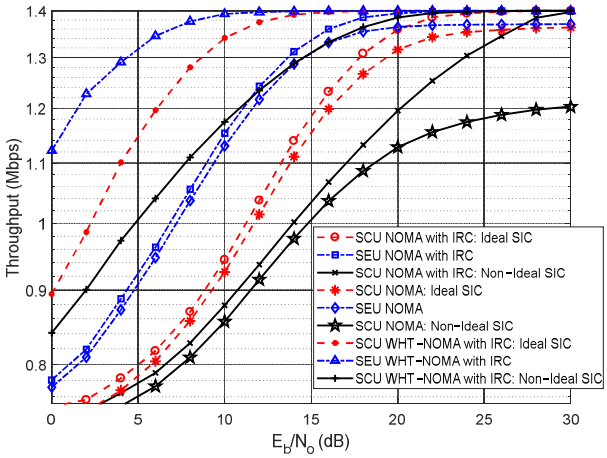

Figure 18. Throughput performance with IRC using BPSK modulation; NOMA Vs. WHT–NOMA, power allocation: SCU = 0.2 and SEU = 0.8.

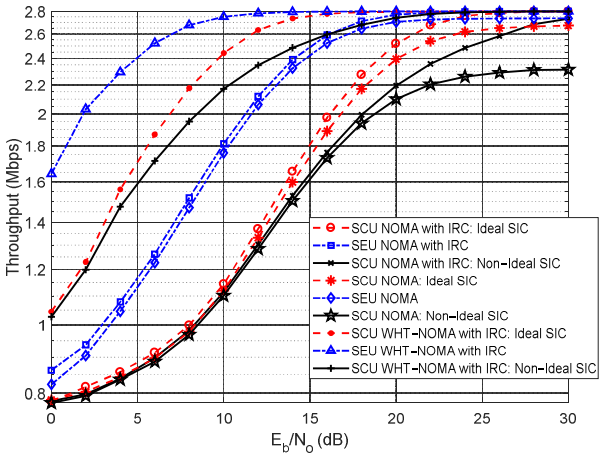

Figure 19. Throughput performance with IRC using QPSK modulation; NOMA Vs. WHT–NOMA, power allocation: SCU = 0.2 and SEU = 0.8.

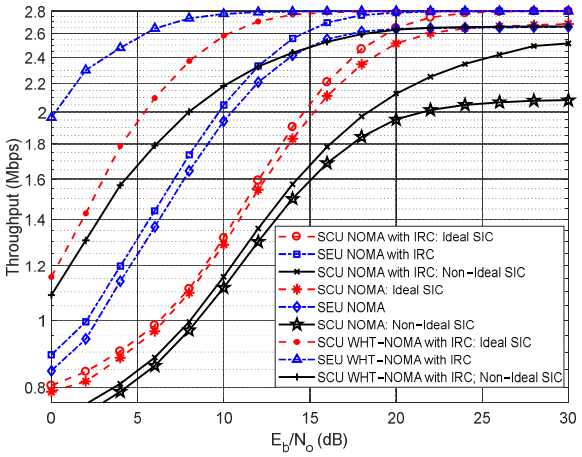

Figure 20. Throughput performance with IRC using QAM modulation; NOMA Vs. WHT–NOMA, power allocation: SCU = 0.2 and SEU = 0.8.

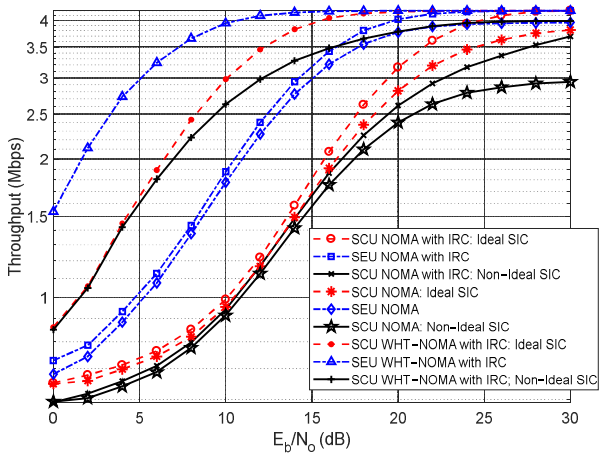

Figure 21. Throughput performance with IRC and 8-QAM modulation; NOMA Vs. WHT–NOMA, power allocation: SCU = 0.2 and SEU = 0.8.

3.3. Computational Complexity Analysis

This section provides the computational complexity analysis of the proposed joint strategy, i.e., WHT+NOMA+IRC, in comparison to the conventional NOMA approach. Computational complexity plays a vital role in analyzing the receiver performance. Theoretically, it is understandable that the complexity of the proposed system in this work should increase with the increment in the number of operations as compared to conventional NOMA. With the inclusion of IRC, the system becomes more complex due to the nature of the IRC weight matrix calculation, given from (34) and (36). Therefore, in this section, the complexity comparison, in terms of the required number of multiplications, is calculated for WHT-NOMA with IRC, compared to conventional NOMA, and is shown in Table 4 and Figure 22 [34,37,10], where N_C represents the number of sub carriers and K represents the number of UEs performing IRC in the small-cell. It is evident from the results in Figure 22 that the computational complexity of the proposed technique is much higher than that of the conventional NOMA approach. Thus, the advantages of better user throughput and reduced BER comes at the expense of higher computational complexity.

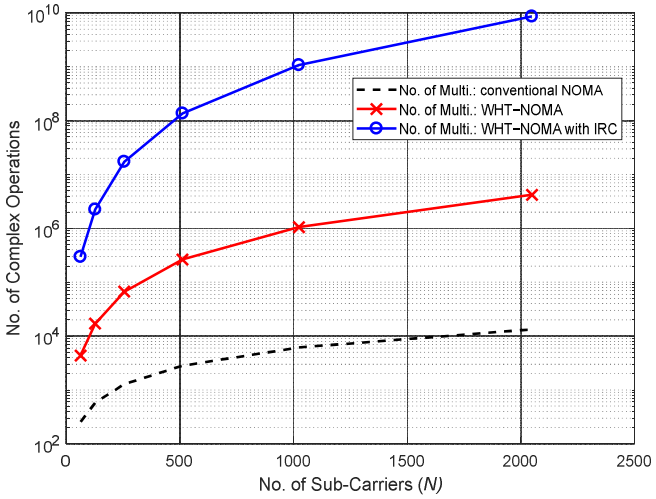

Figure 22. Number of operations for conventional NOMA, WHT-NOMA, and WHT–NOMA–IRC.

Table 4. Computational Complexity [34,37,10].

Complex Operations	NOMA	NOMA + WHT	NOMA + WHT + IRC
Required No. of Multiplications at the Receiver	$\frac{N_C}{2} log_2(N_C)$	$[(N_C/2)\, log_2(N_C)] + [(N_C)^2]$	$[(N_C/2)\, log_2(N_C)] + [(N_C)^2] + \left[2(N_C)^2 + K(N_C)^2 + \left(N_c^3 + 7/2\, N_c{}^2 + 5/2\, N_C - 4\right) + KN_C\right]$

4. Conclusion and Discussion

In this work, a strategy is proposed for the interference management, BER reduction, and throughput enhancement of the small-cell users. Using NOMA in small-cells not only results in better performance gains but also manages the interference by letting the ICI cause MUs to establish connection with the SBS. In the presented scheme, WHT-NOMA provides better throughput and BER performance even at low SNRs as compared to the conventional NOMA. As visible from the simulation analysis in the results section, it is shown that WHT-NOMA can improve the receiver performance gains up to a significant level. The WHT matrix works as a catalyst for the conventional NOMA and improves the BER with a SNR gain of approximately up to 5–10 dB. The receiver design of NOMA needs careful consideration as multiple users are paired together in the power domain, and this creates a lot of interference at the receiver. The presented technique improves BER and throughput performance of both the high- and low-channel-gain small-cell users, i.e., SCUs and SEUs, respectively. Furthermore, the work includes IRC for the ICI suppression, which further reduces the BER of the SUs, resulting in even better user throughput performance as visible from the presented results.

Further, the work can be extended to include interference cancellation techniques like iterative SIC and parallel interference cancellation (PIC). The work may also be extended to the multiuser system level case for checking the scalability performance of WHT-NOMA with IRC in more complex environments. The future extensions can analyze the performance of the proposed method with various transmit and receive diversity techniques such as multiple-input multiple-output (MIMO) NOMA.

Author Contributions: Conceptualization and methodology, M.R.U. and M.A.U.; mathematical modeling, M.R.U., M.A.U. and G.B.S.; data curation and visualization, M.R.U. and M.A.U.; simulation and validation, M.R.U., M.A.U. and R.A.N.; investigation and formal analysis, M.R.U., M.A.U. and G.B.S.; writing—original draft preparation, M.R.U., M.A.U. and R.A.N.; editing, S.Y.S., M.G.M. and C.P.; supervision, S.Y.S., M.G.M. and C.P.; project administration and funding acquisition, S.Y.S. All authors have read and agreed to the published version of the manuscript.

Funding: This work was supported by the National Research Foundation of Korea (NRF) grant funded by the Korea government (MSIT) (No. 2019R1A2C1089542).

Institutional Review Board Statement: Not applicable for studies not involving humans or animals.

Informed Consent Statement: Not applicable for studies not involving humans.

Data Availability Statement: The data presented in this study are available on request from the corresponding author. The data are not publicly available because this work is part of an ongoing funded project.

Conflicts of Interest: The authors declare no conflict of interest.

References

1. Cisco Annual Internet Report (2018–2023) White Paper. Available online: https://www.cisco.com/c/en/us/solutions/collateral/service-provider/visual-networking-index-vni/mobile-white-paper-c11-520862.html (accessed on: 9 October 2020).
2. Al-Turjman, F.; Ever, E.; Zahmatkesh, H. Small cells in the forthcoming 5G/IoT: Traffic modelling and deployment overview. *IEEE Commun. Surv. Tutor.* **2018**, *21*, 28–65.
3. De Ree, M.; Mantas, G.; Radwan, A.; Mumtaz, S.; Rodriguez, J.; Otung, I.E. Key management for beyond 5G mobile small cells: A survey. *IEEE Access* **2019**, *7*, 59200–59236.

4. Usman, M.R.; Usman, M.A.; Shin, S.Y. Channel resource allocation and availability prediction in hybrid access femtocells. *Phys. Commun.* **2017**, *24*, 112–122.
5. Qin, Z.; Yue, X.; Liu, Y.; Ding, Z.; Nallanathan, A. User association and resource allocation in unified NOMA enabled heterogeneous ultra dense networks. *IEEE Commun. Mag.* **2018**, *56*, 86–92.
6. Sano, Y.; Ohwatari, Y.; Miki, N.; Sagae, Y.; Okumura, Y.; Ogawa, Y.; Ohgane, T.; Nishimura, T. Impact on Inter-Cell Interference of Reference Signal for Interference Rejection Combining Receiver in LTE-Advanced Downlink. *IEICE Trans. Commun.* **2012**, *95*, 3728–3738.
7. Léost, Y.; Abdi, M.; Richter, R.; Jeschke, M. Interference rejection combining in LTE networks. *Bell Labs Tech. J.* **2012**, *17*, 25–49.
8. Huang, X.L.; Ma, X.; Hu, F. Machine learning and intelligent communications. *Mob. Netw. Appl.* **2018**, *23*, 68–70.
9. Vamvakas, P.; Tsiropoulou, E.E.; Papavassiliou, S. Dynamic provider selection & power resource management in competitive wireless communication markets. *Mob. Netw. Appl.* **2018**, *23*, 86–99.
10. Ren, B.; Wang, Y.; Sun, S.; Zhang, Y.; Dai, X.; Niu, K. Low-complexity MMSE-IRC algorithm for uplink massive MIMO systems. *Electron. Lett.* **2017**, *53*, 972–974.
11. Tavares, F.M.; Berardinelli, G.; Mahmood, N.H.; Sorensen, T.B.; Mogensen, P. On the impact of receiver imperfections on the MMSE-IRC receiver performance in 5G networks. In Proceedings of the 2014 IEEE 79th Vehicular Technology Conference (VTC Spring), Seoul, Korea, 18–21 May 2014; pp. 1–6.
12. Huang, Y.; Lei, W.; Lu, C.; Berg, M. Fronthaul Functional Split of IRC-Based Beamforming for Massive MIMO Systems. In Proceedings of the 2019 IEEE 90th Vehicular Technology Conference (VTC2019-Fall), Honolulu, HI, USA, 22–25 September 2019; pp. 1–5.
13. Ohwatari, Y.; Morimoto, A.; Miki, N.; Okumura, Y. Investigation on interference rejection combining receiver in heterogeneous networks for LTE-Advanced downlink. In Proceedings of the 2013 IEEE 14th Workshop on Signal Processing Advances in Wireless Communications (SPAWC), Darmstadt, Germany, 16–19 June 2013; pp. 315–319.
14. Wassie, D.A.; Berardinelli, G.; Tavares, F.M.; Tonelli, O.; Sørensen, T.B.; Mogensen, P. Experimental evaluation of interference rejection combining for 5G small cells. In Proceedings of the 2015 IEEE Wireless Communications and Networking Conference (WCNC), New Orleans, LA, USA, 9–12 March 2015; pp. 652–657.
15. Ma, W.; Zhao, H.; Liu, Y.; Shao, S.; Pan, W. A Co-channel interference rejection method for 5G ultra dense heterogeneous networks. In Proceedings of the 2018 IEEE International Conference on Communications Workshops (IEEE ICC Workshops), Kansas City, MO, USA, 20–24 May 2018; pp. 1–5.
16. Usman, M.R.; Khan, A.; Usman, M.A.; Jang, Y.S.; Shin, S.Y. On the Performance of Perfect and Imperfect SIC in Downlink Non Orthogonal Multiple Access (NOMA). In Proceedings of the 2016 International Conference on Smart Green Technology in Electrical and Information Systems (ICSGTEIS), Bali, Indonesia, 6–8 October 2016; pp. 102–106.
17. Ding, Z.; Liu, Y.; Choi, J.; Sun, Q.; Elkashlan, M.; Chih-Lin, I.; Poor, H.V. Application of non-orthogonal multiple access in LTE and 5G networks. *IEEE Commun. Mag.* **2017**, *55*, 185–191.
18. Li, A.; Lan, Y.; Chen, X.; Jiang, H. Non-orthogonal multiple access (NOMA) for future downlink radio access of 5G. *China Commun.* **2015**, *12*, 28–37.
19. Mohammadi, M.; Shi, X.; Chalise, B.K.; Ding, Z.; Suraweera, H.A.; Zhong, C.; Thompson, J.S. Full-duplex non-orthogonal multiple access for next generation wireless systems. *IEEE Commun. Mag.* **2019**, *57*, 110–116.
20. Vaezi, M.; Schober, R.; Ding, Z.; Poor, H.V. Non-orthogonal multiple access: Common myths and critical questions. *IEEE Wirel. Commun.* **2019**, *26*, 174–180.
21. Liu, J.; Wu, G.; Xiao, S.; Zhou, X.; Li, G.Y.; Guo, S.; Li, S. Joint power allocation and user scheduling for device-to-device-enabled heterogeneous networks with non-orthogonal multiple access. *IEEE Access* **2019**, *7*, 62657–62671.
22. Zhang, S.; Zhang, N.; Kang, G.; Liu, Z. Energy and spectrum efficient power allocation with NOMA in downlink HetNets. *Phys. Commun.* **2018**, *31*, 121–132.
23. Forouzesh, M.; Azmi, P.; Mokari, N.; Wong, K.K.; Pishro-Nik, H. Robust Physical Layer Security for Power Domain Non-Orthogonal Multiple Access-Based HetNets and HUDNs: SIC Avoidance at Eavesdroppers. *IEEE Access* **2019**, *7*, 107879–96.
24. Tang, R.; Cheng, J.; Cao, Z. Contract-based incentive mechanism for cooperative NOMA systems. *IEEE Commun. Lett.* **2018**, *23*, 172–175.
25. Diamanti, M.; Fragkos, G.; Tsiropoulou, E.E.; Papavassiliou, S. Unified User Association and Contract-Theoretic Resource Orchestration in NOMA Heterogeneous Wireless Networks. *IEEE Open J. Commun. Soc.* **2020**, *1*, 1485–1502.
26. Zhang, Y.; Zhu, Y.; Xia, W.; Shen, F.; Zuo, X.; Yan, F.; Shen, L. Game-based power control for downlink non-orthogonal multiple access in HetNets. In Proceedings of the 2018 IEEE Global Communications Conference (GLOBECOM), Abu Dhabi, United Arab Emirates, 9–13 December 2018; pp. 206–212.
27. Song, Z.; Ni, Q.; Sun, X. Distributed power allocation for non-orthogonal multiple access heterogeneous networks. *IEEE Commun. Lett.* **2018**, *22*, 622–625.
28. Nasser, A.; Muta, O.; Elsabrouty, M.; Gacanin, H. Interference mitigation and power allocation scheme for downlink MIMO–NOMA HetNet. *IEEE Trans. Veh. Technol.* **2019**, *68*, 6805–6816.

29. Iossifides, A.C. Optimum Detection of Walsh-Hadamard Multiplexed Antipodal Signals over Rayleigh Fading Channels. In Proceedings of the IEEE 18th International Conference on Telecommunications (ICT), Ayia Napa, Cyprus, 8–11 May 2011; pp. 282–287.
30. Siadari, T.S.; Shin, S.Y. Joint Hadamard transform and Alamouti scheme for wireless communication system. *Aeu-Int. J. Electron. Commun.* **2014**, *68*, 889–891.
31. Khan, A.; Arif, A.; Nawaz, T.; Baig, S. Walsh Hadamard transform based transceiver design for SC-FDMA with discrete wavelet transform. *China Commun.* **2017**, *14*, 193–206.
32. Irfan, M.; Shin, S.Y. Robust Walsh–Hadamard transform-based spatial modulation. *Digit. Signal. Process.* **2017**, *64*, 1–7.
33. Usman, M.R.; Khan, A.; Usman, M.A.; Shin, S.Y. Joint non-orthogonal multiple access (NOMA) & Walsh-Hadamard transform: Enhancing the receiver performance. *China Commun.* **2018**, *15*, 160–177.
34. Khan, A.; Khan, S.; Baig, S.; Asif, H.M.; Shin, S.Y. Wavelet OFDM with Overlap FDE for non-Gaussian channels in precoded NOMA based systems. *Future Gener. Comput. Syst.* **2019**, *97*, 165–179.
35. 3GPP, R1-111562. *Interference Aware Receiver Modeling at System Level*; Renesas Mobile Europe Ltd.: 2011. Available online: https://www.3gpp.org/DynaReport/TDocExMtg--R1-66--28505.htm (accessed on: 1 Mach 2020)
36. Su, X.; Yu, H.; Kim, W.; Choi, C.; Choi, D. Interference cancellation for non-orthogonal multiple access used in future wireless mobile networks. *EURASIP J. Wirel. Commun. Netw.* **2016**, *2016*, 231.
37. Zhang, X. *Matrix Analysis and Applications*; Tsinghua University Press: Beijing, China, 2004.